Robustness of persistent currents in two-dimensional Dirac systems with disorder

Lei Ying[1] and Ying-Cheng Lai[1,2,*]

[1]*School of Electrical, Computer, and Energy Engineering, Arizona State University, Tempe, Arizona 85287, USA*

[2]*Department of Physics, Arizona State University, Tempe, Arizona 85287, USA*

(Received 7 November 2016; revised manuscript received 8 August 2017; published 5 October 2017)

We consider two-dimensional (2D) Dirac quantum ring systems formed by the infinite mass constraint. When an Aharonov-Bohm magnetic flux is present, e.g., through the center of the ring domain, persistent currents, i.e., permanent currents without dissipation, can arise. In real materials, impurities and defects are inevitable, raising the issue of robustness of the persistent currents. Using localized random potential to simulate the disorder, we investigate how the ensemble-averaged current magnitude varies with the disorder density. For comparison, we study the nonrelativistic quantum counterpart by analyzing the solutions of the Schrödinger equation under the same geometrical and disorder settings. We find that, for the Dirac ring system, as the disorder density is gradually increased, the average current decreases slowly initially and then plateaus at a finite nonzero value, indicating remarkable robustness of the persistent currents. The physical mechanism responsible for the robustness is the emergence of a class of boundary states—whispering gallery modes. In contrast, in the Schrödinger ring system, such boundary states cannot form, and the currents diminish rapidly to zero with an increase in the disorder density. We develop a physical theory based on a quasi-one-dimensional approximation to understand the striking contrast in the behaviors of the persistent currents in the Dirac and Schrödinger rings. Our 2D Dirac ring systems with disorder can be experimentally realized, e.g., on the surface of a topological insulator with natural or deliberately added impurities from the fabrication process.

DOI: 10.1103/PhysRevB.96.165407

I. INTRODUCTION

Persistent or permanent currents, i.e., currents requiring no external voltage with zero resistance, were traditionally thought to occur only in superconductors. However, about three decades ago, it was theoretically predicted [1] that such dissipationless currents can emerge in normal metallic or semiconductor ring systems subject to a central Aharonov-Bohm (AB) [2] magnetic flux. In particular, if the ring size is smaller than the elastic scattering length, the electron motion in the entire domain will become ballistic, effectively eliminating scattering. If the ring size is larger than the elastic scattering length, the electron's behavior will be diffusive with a current proportional to $1/\tau_D$, where τ_D is the diffusion time around the ring. While the environmental temperature needs to be sufficiently low to reduce inelastic scattering from phonon-electron and/or electron-electron interactions for the currents to be observed [1,3–5], the metallic material itself remains "normal" (i.e., not superconducting). The remarkable phenomenon of persistent currents was subsequently observed experimentally in a large variety of settings [6–13], all being nonrelativistic quantum systems.

Persistent currents in nonrelativistic quantum systems are vulnerable to material impurities, which fundamentally restricts the phenomenon to systems at or below the mesoscopic scale. Indeed, in real materials disorder is inevitable, which can dramatically reduce the phase coherent length and the elastic scattering length due to enhanced random scattering. In general, random disorder can remove the energy degeneracies and induce level repulsion, opening energy gaps and destroying the conducting state. As a result, disorder in metallic or semiconductor systems [one- or two-dimensional (1D or 2D)] tends to diminish the persistent currents [14–20]. As the strength of the disorder is increased, the currents decay exponentially to zero [14,20].

Recent years have witnessed a tremendous development and growth of interest in 2D Dirac materials such as graphene [21–27], topological insulators [28], molybdenum disulfide (MoS_2) [29,30], HITP [$Ni_3(HITP)_2$] [31], and topological Dirac semimetals [32–36]. The quantum physics of these 2D materials is governed by the Dirac equation or the generalized Dirac-Weyl equation [37,38], and there were studies of persistent currents, e.g., in graphene [39–48] and other Dirac materials [49,50]. The effects of boundary deformation on the persistent currents were recently investigated [51,52], where it was found that, even when the deformation is so severe that the corresponding classical dynamics in the 2D domain becomes fully chaotic, persistent currents can sustain. The physical origin of the so-called superpersistent currents [51,52] can be attributed to the emergence and robustness of a type of quantum states near the boundaries of the domain, which carry a large angular momentum and correspond essentially to the whispering gallery modes (WGMs) that arise commonly in optical systems [53–56] and can occur in nonrelativistic quantum electronic systems [57] as well. The Dirac WGMs are insensitive to boundary deformations, which may be intuitively understood as a consequence of the zero flux boundary condition required for nontrivial, physically meaningful solutions of the Dirac equation. In spite of these efforts, the effects of bulk disorder on persistent currents in 2D Dirac systems remain an open issue. In particular, since there are random scattering sources inside the domain with a finite probability of occurrence even near the boundary, it is not intuitively clear whether the Dirac WGMs and hence persistent currents can still exist when there are random impurities in the ring domain.

*ying-cheng.lai@asu.edu

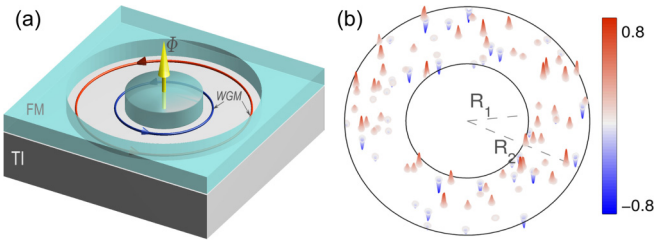

FIG. 1. (a) Schematic illustration of a ring domain with an AB magnetic flux through the center. The light blue color denotes the regions of infinite mass. Red and blue loops illustrate the eigenstates near the outer and inner boundaries, respectively. (b) Schematic illustration of random disorder uniformly distributed in the ring region, with their strength denoted with different colors. Experimentally, a Dirac ring can be generated by placing a ferromagnetic insulator of proper shape on the surface of a topological insulator [51,52].

In this paper, we investigate the effects of random disorder on persistent currents in 2D relativistic quantum systems. To be concrete, we consider a Dirac ring domain with a vertical magnetic flux through the center, as shown in Fig. 1(a). To completely constrain a Dirac fermion within the domain, we impose the infinite mass boundary condition originally introduced by Berry [58] into the study of chaotic neutrino billiards, which is experimentally realizable through a proper arrangement of ferromagnetic insulation [59]. We assume uncorrelated disorder throughout the domain, which can be simulated using localized, random electric potential uniformly distributed in the domain, as illustrated in Fig. 1(b). In an experiment, for a given material, neither the strength nor the density of the disorder can be readily adjusted. However, the sample size can be controlled. Classically, under a vertical magnetic field, the electrons move along circular trajectories in the domain. In experiments, for a larger ring sample with constant disorder density, an electron encounters more disorder/scattering events in one complete rotation. For computational convenience, we fix the outer radius of the ring domain to be unity. In this case, varying the disorder density is equivalent to changing the size of ring domain, where a higher density corresponds to a larger domain. Following this heuristic consideration, we fix the disorder strength as well as the domain size but systematically vary the density of the disorder. For convenience, in our computations we set the total number of disorders in the whole domain as a control parameter, and we solve the Dirac equation to obtain the magnitudes of the persistent currents as a function of the number of disorders. For comparison with the nonrelativistic quantum counterpart, we solve the Schrödinger equation under the same setting. Our main results are the following. For the Dirac ring system, as the number of disorders is systematically increased, the average current decreases slowly initially and then plateaus at a finite nonzero value, indicating that the persistent currents are robust. We demonstrate that WGMs are the physical mechanism responsible for the robust currents. In contrast, in the nonrelativistic quantum ring system, the WGMs are sensitive and fragile to the disorders, leading to a rapid and exponential decay of the currents to zero. We develop a physical theory based on a quasi-one-dimensional approximation to understand the strikingly contrasting behaviors of the currents in the Dirac and Schrödinger rings. An important implication of our finding is that persistent currents in the Dirac rings can occur in realistic systems of large size.

In Sec. II, we describe the Hamiltonian for a 2D Dirac ring and the numerical method to calculate the persistent currents. In Sec. III, we demonstrate the robustness of the currents against random disorders and the emergence of WGMs. In Sec. IV, we justify our use of the quasi-1D approximation and derive a physical theory to understand the drastically contrasting decaying behaviors in Dirac and Schrödinger ring systems. In Sec. V, we present conclusions and a discussion about the possibility of observing persistent currents in Dirac systems of large size (e.g., beyond the mesoscopic scale).

II. MODEL HAMILTONIAN AND SIMULATION SETTING

We consider a 2D Dirac ring domain where an AB magnetic flux passes through the central region, as shown schematically in Fig. 1(a). The Dirac Hamiltonian subject to a magnetic field is

$$\mathcal{H} = \mathcal{H}_0 + U(\boldsymbol{r}) = \hbar v(\hat{\boldsymbol{p}} + e\boldsymbol{A})\cdot\hat{\boldsymbol{\sigma}} + V(\boldsymbol{r})\sigma_z + U(\boldsymbol{r}), \quad (1)$$

where $\hat{\boldsymbol{p}} = -i\hbar\partial/\partial\mathbf{r}$ is the momentum operator, $\hat{\boldsymbol{\sigma}} = [\sigma_x,\sigma_y,\sigma_z]^T$ is the "vector" of Pauli matrices, $\boldsymbol{A} = \Phi\partial(-\ln|\boldsymbol{r}|)/\partial\boldsymbol{r}$ is the magnetic vector potential, and Φ is the AB magnetic flux. The disorders are modeled as a random electrical potential function $U(\boldsymbol{r})$, and the mass potential that confines the Dirac particle in the domain is $V(\mathbf{r})$, where $V = \infty$ for $r < R_1$ or $r > R_2$. In the polar coordinates, the stationary Dirac equation in the ring domain can be written as (in the units $\hbar = v = 1$)

$$\begin{pmatrix} i[U(r,\theta)-\varepsilon] & e^{-i\theta}\left(\partial_r - \frac{i}{r}\partial_\theta + \frac{\Phi/\Phi_0}{r}\right) \\ e^{i\theta}\left(\partial_r + \frac{i}{r}\partial_\theta - \frac{\Phi/\Phi_0}{r}\right) & i[U(r,\theta)-\varepsilon] \end{pmatrix}\Psi(r,\theta) = 0, \quad (2)$$

where ε denotes the eigenenergy, the relevant lengths are normalized by the outer radius R_2 (e.g., the inner radius becomes $\xi = R_1/R_2$), and $\Phi_0 = h/e$. In the absence of random disorders, the Dirac equation in the ring domain can be solved analytically with the following solutions:

$$\begin{aligned}\Psi(r,\theta) &= [\psi^-(r,\theta),\psi^+(r,\theta)]^T \\ &= e^{im\theta}[e^{-i\theta/2}\chi^-_{\bar{m}}(r), ie^{i\theta/2}\chi^+_{\bar{m}}(r)]^T, \end{aligned} \quad (3)$$

where $\bar{m} = m + \Phi/\Phi_0$ is the effective quantum number of the angular momentum and $m = \pm 1/2, \pm 3/2, \pm 5/2, \ldots$ are the eigenvalues of the operator $\hat{\mathcal{J}}_z = -i\partial_\theta + \sigma_z$. Differing from the hard potential boundary condition in the Schrödinger system, which is given by $\psi(r=\xi,\theta) = \psi(r=1,\theta) = 0$, the infinite mass boundary condition in the Dirac system leads to the following relation between the two components of the spinor wave function [58]:

$$\psi^+/\psi^- = i\,\mathrm{sgn}[V]e^{i\theta}. \quad (4)$$

The radial part of the whole wave function can be expressed as a set of Hankel functions [see Eq. (A3) in Appendix A].

Treating the random disorders as perturbations, we have

$$\sum_{i,j}\langle j|\mathcal{H}|i\rangle = \sum_i E_i^{(0)} + \sum_{i,j}\langle j|U(r,\theta)|i\rangle, \tag{5}$$

where $E_i^{(0)}$ and $|i\rangle$'s are the eigenvalues and eigen wave functions of the unperturbed Hamiltonian $H_0 = H_{U=0}$, respectively. The energy levels of the perturbed system can be solved numerically using the Hamiltonian in Eq. (5).

The concrete parameter setting in our simulation is the following. We model the random disorders through a set of uncorrelated Gaussian potential functions:

$$U(r,\theta) = \sum_{s=1}^{N} U_s(r_s,\theta_s) = \sum_{s=1}^{N} u_s e^{-\delta r^2/2\sigma^2},$$

where s and N are the index and the total number of random impurities in the domain, and σ and u_s are the size and the potential height of a single electric impurity, respectively. We set the cutoff radius of any disorder to be $\delta r \leqslant 3\sigma$ and the mean radius of the disorders to be $(R_2 - R_1)/20$. The strength of the disorders is randomly chosen from the interval $[-u_m/2, u_m/2]$, where u_m is determined in terms of the average spacing of the first ten energy levels, ΔE_{10}.

Note that our computations are based on the Dirac equation (not the tight-binding model), so in principle the number of energy levels is infinite. For high energies, the spacing between two adjacent levels tends to be uniform. To be concrete, we focus on the low energy regime and perform detailed computations for 10 representative levels.

For convenience, we use the superscripts "D" and "S" to denote the results for the Dirac and Schrödinger ring domains, respectively. Our computation gives $\Delta E_{10}^{(S)} \approx 10\Delta E_{10}^{(D)}$ for $\xi = 1/2$. The maximum number of disorders is chosen to be 500 (corresponding to impurity area ratio $S_{\rm dis}/S_{\rm ring} \simeq 0.43$) to prevent them from covering the ring domain completely. The single-level persistent current is conventionally defined as [60]

$$I_n = \sqrt{\langle I_n^2(\Phi)\rangle}, \tag{6}$$

where $I_n(\Phi) = -\partial E_n(\Phi)/\partial\Phi$ is the flux-dependent persistent current associated with the nth energy level and $\langle\cdots\rangle$ denotes disorder averaging. The experimentally measurable persistent current is given by [3,60]

$$I^{\rm typ}(\Phi) = \sqrt{\left\langle\left[\sum_{n=1}^{n_F} I_n(\Phi)\right]^2\right\rangle}, \tag{7}$$

where n_F is the maximum energy level below the Fermi energy. The average persistent currents over magnetic flux are written as $I^{\rm typ} = \overline{I^{\rm typ}(\Phi)}$. Generally, the persistent currents in Eqs. (6) and (7) are normalized by the corresponding disorder-free currents I_n^0 and I^0, respectively. Note that the magnitudes of the edge currents are different, which gives rise to a net current.

III. RESULTS AND QUALITATIVE UNDERSTANDING

Figures 2(a) and 2(b) show, for the Dirac and Schrödinger systems, respectively, the typical single-level persistent currents versus the number N of random disorders, which are calculated using 10^2 statistical realizations. The error in the calculated value of the current amplitude is about 10^{-2}. In both cases, the current amplitude decays exponentially for $0 < N \lesssim 350$ (i.e., $0 < S_{\rm dis}/S_{\rm ring} \lesssim 0.3$): $I_n \sim I_n^0 \exp[-\gamma^{(D,S)}N]$, with the distinct feature that the decay rate for the Dirac system is about half of that for the Schrödinger system: $\gamma^{(D)}/\gamma^{(S)} \approx 1/2$. A more remarkable feature is that, for the Dirac system, after an initial exponential decay, the current amplitude approaches a constant value of about 10^{-1} (which is about one order of magnitude larger than the numerical error) for $N \geqslant 350$, but for the corresponding Schrödinger system the current amplitude effectively decays to zero. We see that, as more random disorders are introduced into the domain (or equivalently, as the domain size is increased), the decaying behavior of the persistent currents is characteristically different for the Dirac and Schrödinger systems: for the former the currents are robust and continue to exist (in spite of deterioration in the amplitude), but for the latter the currents quickly diminish. That is, persistent currents in the Dirac system are robust against random disorders. The decay behaviors of the average persistent current associated with the five lowest energy levels for both the Dirac and Schrödinger rings are demonstrated in Fig. 2(c).

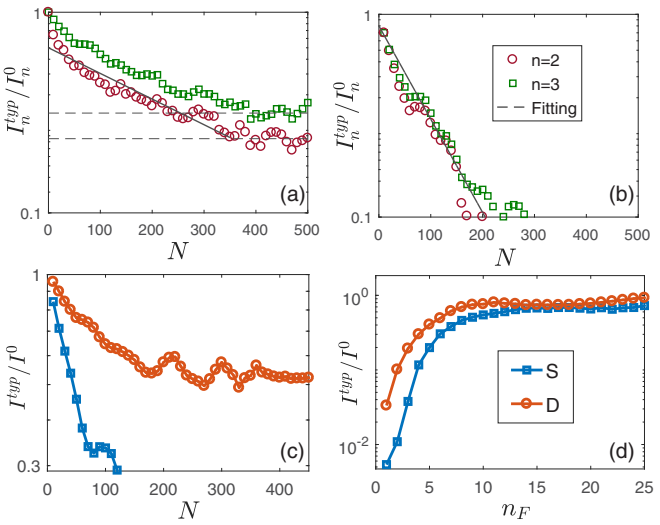

FIG. 2. Typical single-level persistent currents vs the number of the disorders for (a) Dirac and (b) Schrödinger rings, for fixed disorder strength $u_m^{(D,S)} = 300\Delta E_{10}^{(D,S)}$. The mean radius of a single impurity is $\delta r = (1-\xi)/20$. (c) The average persistent current vs the number of disorders for five levels below the Fermi energy, where other parameters are the same as in (a), (b) for the Dirac (denoted as "D" and illustrated as circles) and Schrödinger (denoted as "S" and displayed as squares) rings. The range of the number of disorders, $N \in [0,500]$, corresponds to the range of the ratio between the disorder and ring areas, $S_{\rm dis}/S_{\rm ring} \in [0,0.43]$. (d) Total persistent current vs n_F, the number of levels below the Fermi energy, for the Schrödinger (blue squares) and Dirac (red circles) ring systems, where the number of impurities is 400.

The behavior of the total persistent current versus n_F, the number of levels below the Fermi energy, is shown in Fig. 2(d), where there are 400 random impurities in the ring domain for both the Schrödinger (blue squares) and Dirac (red circles) cases. The quantity n_F is increased from 1 to the value when the total persistent current is saturated. The currents for both systems increase with n_F for $n_F \in [1,10]$ and

become plateaued for further increase in the value of n_F. In the increasing phase, the persistent current of the Dirac ring system is much larger than that of the Schrödinger counterpart (note the logarithmic scale for the current). That is, for low energy levels (e.g., $n_F \leqslant 10$), disorders have a more devastating effect on the total persistent current for the Schrödinger system. However, the saturated current value for the Dirac ring is not significantly larger than that for the Schrödinger system (again note the logarithmic scale) because the contributions to the total current from higher energy levels are less sensitive to disorders than those from the low energy levels.

One question is whether Klein tunneling is responsible for the robust persistent currents in the Dirac ring system. In relativistic quantum systems, Klein tunneling is referred to as the phenomenon where an incoming electron can penetrate a potential barrier whose height is larger than the electron energy with probability 1 [61]. In 1D systems with random impurities, Klein tunneling has a strong manifestation in the behavior of the persistent currents [62]. This is because, in one dimension, the incident "angle" of a wave on an impurity is zero so that the condition for Klein tunneling is always met. However, in two dimensions, there can be a wide distribution of the incident angle [61] on a random potential, and the angle range for Klein tunneling is quite limited. In our setting, the potential field of an electric disorder is Gaussian, rendering Klein tunneling highly unlikely. To provide further evidence that Klein tunneling plays little role in sustaining the persistent currents in the Dirac ring system with disorders, we set the impurity potential to be attractive in the range $[-u_m,0]$ so that no Klein tunneling can occur. We obtain essentially the same result as in Fig. 2(a).

The physical mechanism for persistent currents to sustain in the Dirac ring system with random disorders can be attributed to a set of WGM states near the domain boundaries. This can be verified by examining the local density of states (LDS) and the local current density (LCD) that can be calculated [58] as $\boldsymbol{j}(r,\theta) = \Psi^{\dagger}(r,\theta)\hat{\boldsymbol{\sigma}}\Psi(r,\theta)$. The LDS and LCD distributions are shown in Fig. 3, where the WGM characteristics of the boundary states are apparent. In general, a Dirac fermion tends to stay near one of the infinite mass boundaries with a high probability, due to the zero-flux boundary condition. For a Dirac ring domain without any random disorder, the intrinsic circular symmetry stipulates an identical radial wave function for different angular modes, i.e., the Hankel functions with different angular momentum quantum numbers. In this case, the WGMs tend to be "attached" to the boundaries of the ferromagnetic material. As a result, there is an asymmetry in the plot of the energy levels versus the magnetic flux, as shown Fig. 3(a). Random disorders break the circular symmetry, and, as a result, the WGMs tend to be detached from the boundaries, but they are still near them. In general, the LDS and LCD patterns depend on the wave vector and the detailed distribution of the random disorders. For comparison, we also plot the LDS and LCD patterns for the Schrödinger ring, where the LCD is calculated by $\boldsymbol{j}(r,\theta) = \Psi^{\dagger}(r,\theta)(\hat{\boldsymbol{\nabla}} + \boldsymbol{A})\Psi(r,\theta)$. As shown in Figs. 3(e) and 3(f), the LCD is highly localized due to the disorders.

To further understand the robustness of the WGMs in the Dirac ring domain against random disorders, we examine the wave functions at higher energy levels. Without any disorder, while the LDS pattern "attaches" to the boundary, its radial

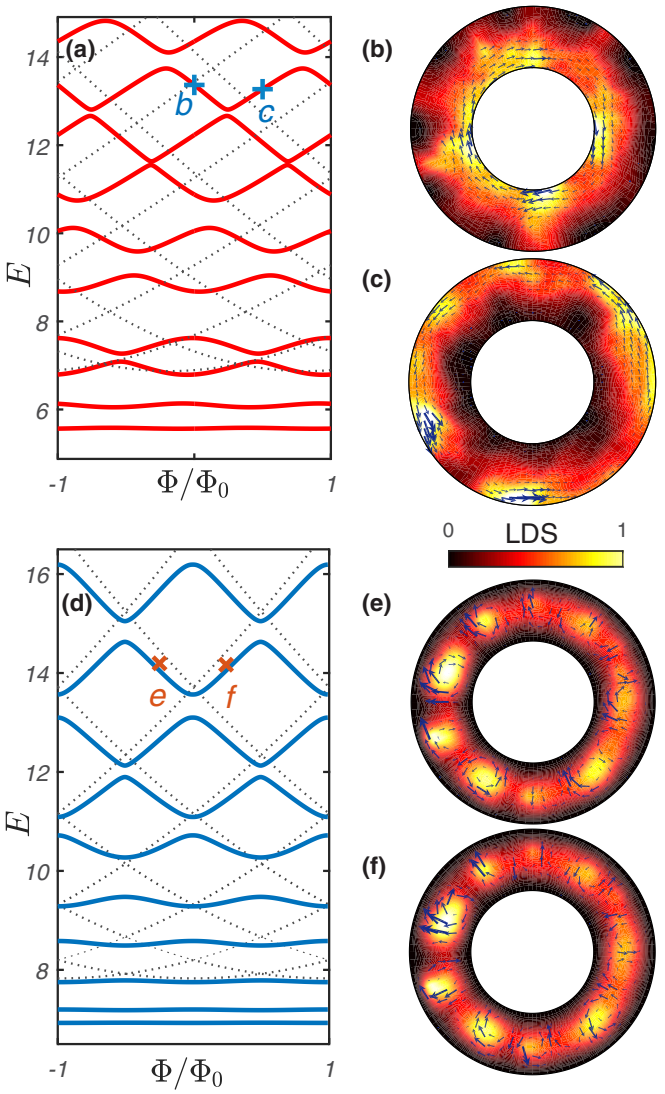

FIG. 3. (a) Energy level vs the strength of the magnetic flux for the Dirac system. Gray dashed curves are for the case without random disorders, and the solid curves represent the energy levels with 100 random disorders [(b) and (c) are for the ninth energy level in the disordered system]. LDS and LCD patterns are shown for the outer (b) and inner (c) states. The locations of the states in (b) and (c) are indicated by the crosses in (a). (d)–(f) Energy level vs the strength of the magnetic flux and the LDS and LCD patterns for the Schrödinger system. The locations of the states in (e) and (f) are indicated by the crosses in (d).

wave function of high levels ($n \geqslant 9$) is typically maximized in the interior of the domain, as shown by the dashed black curves in Fig. 4. Random disorders attenuate the LDS in the interior region, but its values remain significant near the boundaries, as shown by the solid curves in Figs. 4(a) and 4(b). For the Schrödinger system, as shown in Figs. 4(c) and 4(d), the disorders have little effect on the pattern of the average radial wave function. However, the azimuthal components of the wave functions are affected [cf., the 2D LDS patterns in Figs. 3(e) and 3(f)].

A fundamental feature of the Dirac system, which is absent in the Schrödinger counterpart, is the spin texture. We find that

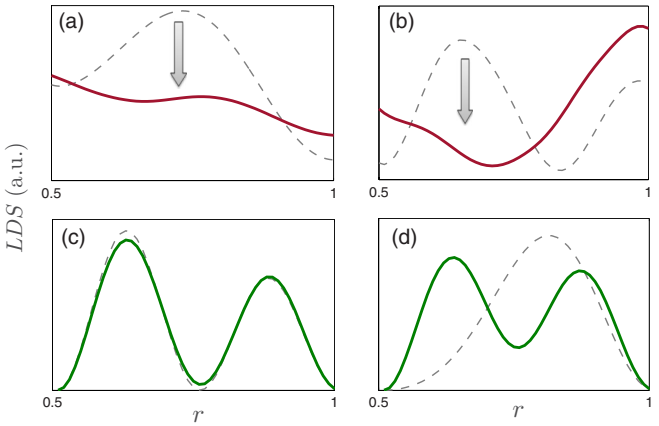

FIG. 4. (a), (b) The radial wave functions of the "clean" Dirac systems (gray dashed) of the 22nd and the 25th levels, respectively. The solid curves in (a), (b) show the corresponding average radial wave functions for the case in which there are 100 random disorders in the domain. (c), (d) The radial wave functions of the Schrödinger system with the same parameters as (a), (b). Green solid and gray dashed curves denote the disordered influenced and the "clean" wave functions, respectively.

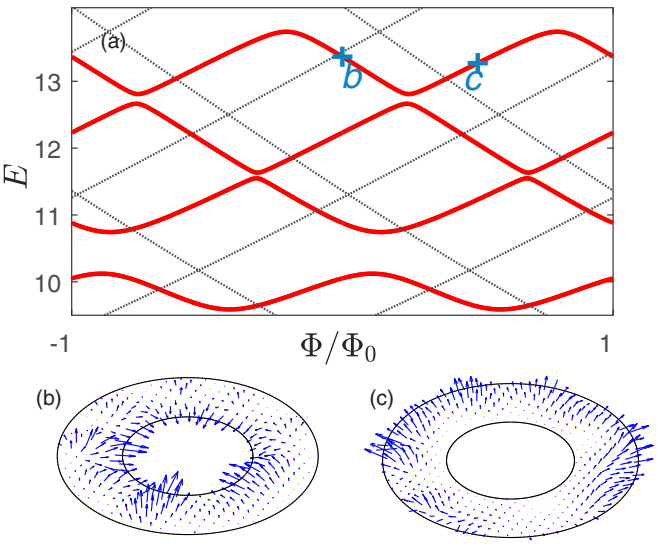

FIG. 5. For the Dirac ring system, the spin orientations corresponding to the LDS patterns in Figs. 3(a)–3(c). The locations of the states in (b) and (c) are indicated by the crosses in (a). Both states correspond to the ninth level, as in Fig. 3.

the spin texture associated with the WGMs is hardly affected by the random disorders. For a 2D Dirac system (e.g., the surface of a 3D topological insulator), the spin orientation is given by [63] $\boldsymbol{s}(r,\theta) = \Psi^{\dagger}(r,\theta)\hat{\boldsymbol{S}}\Psi(r,\theta)$, with $\hat{\boldsymbol{S}} = (1/2)(\sigma_y, -\sigma_x, \sigma_z)$. As shown in Fig. 5, the spin orientations of the WGMs near the inner and outer boundaries tend to be parallel to their respective normal vectors. (For nonboundary states, the spin orientations are random.) The robustness of the spin orientation against random disorders can again be attributed to the zero-flux boundary condition that allows the states with a definite spin orientation to close on itself after completing a circular path to ensure constructive interference. That is, the infinite mass boundaries in the Dirac system tend to "protect" the spin orientation for the WGM type of boundary states.

IV. PHYSICAL UNDERSTANDING OF THE ROBUST PERSISTENT CURRENTS IN THE DIRAC RING

For a circular Dirac domain, in the absence of random disorders the energy level ε depends on the angular momentum quantum number m: $\varepsilon = \varepsilon(m)$. If the thickness of the quantum ring is not large, as an approximation [64] we can assume that the disorders have little effect on the radial component $\chi(r)$ of the eigenfunctions, but they can affect significantly the azimuthal component $\phi(\theta)$. A general wave function from the Dirac equation can be written as a linear combination of the eigenfunctions: $\Psi(r,\theta) = \sum_n \phi_n(\theta)\chi_n(r)$, where $\chi_n(r)$ is the eigenfunctions of the Bessel's differential equation (see Appendix A for details), and $\phi_n(\theta)$ is the azimuthal wave function associated with the original angular momentum quantum number m in the absence of disorders. The orthogonality condition for $\chi^{\pm}_{n,m}(r)$ is (Appendixes A and B)

$$\int_{\xi}^{1} dr \frac{1}{r} \chi^{\pm *}_{n',m}(r)\chi^{\pm}_{n,m}(r) = \delta_{n',n}.$$

Utilizing this condition and eliminating the radial partial terms in Eq. (2), we obtain the governing equation for the quasi-1D azimuthal wave function as

$$\partial_\theta \phi_{n,m}(\theta) = \hat{\mathcal{G}}\phi_{n',m}(\theta), \tag{8}$$

$$\hat{\mathcal{G}} = i \sum_s \sum_{n'} \begin{pmatrix} m - 1/2 & -e^{-i\theta}\Gamma^{(s)}_{nn',m} \\ -e^{i\theta}\Gamma^{(s)}_{nn',m} & m + 1/2 \end{pmatrix}, \tag{9}$$

where s is the index of the random disorders, n and n' are the energy level indices, and $\Gamma^{(s)}_{nn',m}$ is the scattering integral associated with the radial component, which is given by

$$\begin{aligned} \Gamma^{(s)}_{nn',m}(r_s) &= -\int_{\xi}^{1} \chi^{-*}_{n,m}(r)U_s(r,\theta)\chi^{+}_{n',m}(r)dr \\ &= \int_{\xi}^{1} \chi^{+*}_{n,m}(r)U_s(r,\theta)\chi^{-}_{n',m}(r)dr. \end{aligned} \tag{10}$$

The approximation procedure is schematically illustrated in Fig. 6(a), with two representative radial wave functions in Figs. 6(b) and 6(c), respectively. For simplicity, we set the potential characterizing the random disorders as

$$U(r,\theta) = \sum_s U_s(r_s,\theta_s) = \sum_s (u_s/r)\delta(r - r_s)\delta(\theta - \theta_s),$$

which yields

$$\Gamma^{(s)}_{nn',m} = -u_s \chi^{-*}_{n,m}(r_s)\chi^{+}_{n',m}(r_s)\delta(\theta - \theta_0).$$

For comparison with the nonrelativistic quantum counterpart, we note that for a Schrödinger domain, the azimuthal equation is [64]

$$\left(\partial^2_\theta + m^2\right)\phi_n(\theta) = \sum_s \sum_{n'} \Gamma^{(s)}_{n'n,m}\phi_{n'}(\theta),$$

where

$$\Gamma^{(s)}_{n'n,m} = u_s \chi^{*}_{n',m}(r_s)\chi_{n,m}(r_s)\delta(\theta - \theta_s).$$

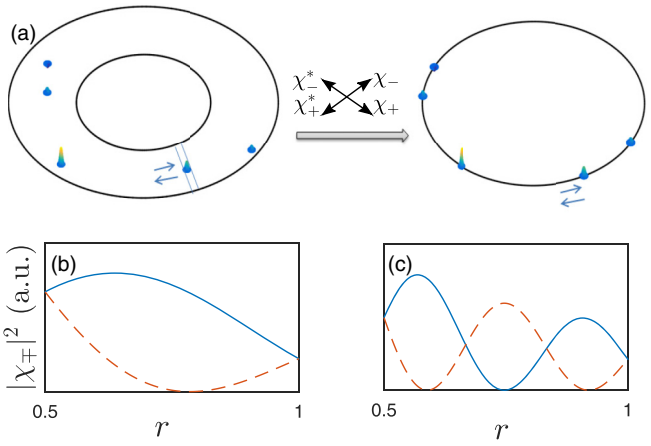

FIG. 6. (a) Schematic illustration of the quasi-one-dimensional model by integrating over the radial dimension. The integral is over a multiplication of the upper and lower components of the radial wave functions, as indicated in (a). (b), (c) The upper (solid) and lower (dashed) radial wave functions for the 11th and 15th energy levels, respectively.

Having obtained a quasi-1D equation that approximately describes the effects of the random impurities, Eq. (8), we are in a position to set up a quantum transport model based on the transfer-matrix approach. In particular, the transfer operator $\mathcal{T}$ for one complete rotation in the ring domain subject to random impurities is defined as [65,66]

$$\phi(\theta = 2\pi) = \mathcal{T}\phi(\theta = 0), \tag{11}$$

with

$$\mathcal{T} = \mathcal{T}_P^{(N+1)} \prod_{s=N}^{1} \mathcal{T}_M^{(s)} \mathcal{T}_P^{(s)}, \tag{12}$$

where the operators $\mathcal{T}_P^{(s)}$ and $\mathcal{T}_M^{(s)}$ represent the propagating and scattering processes. The operators can be obtained from the first-order Neumann solution [67–69] of the azimuthal Dirac equation (8) as

$$\phi(\theta_{s'}) = \hat{\mathcal{Q}} \exp\left[\int_{\theta_s}^{\theta_{s'}} \hat{\mathcal{G}}(\theta) d\theta\right] \phi(\theta_s), \tag{13}$$

with $\hat{\mathcal{Q}}$ denoting the Dyson ordering operator and $\hat{\mathcal{G}}$ being an angle-dependent operator. Analytically, it is infeasible to obtain the solutions of Eq. (13). To gain insights, we set $\hat{\mathcal{Q}} = 1$ to obtain the following expressions:

$$\mathcal{T}_P^{(s)} = \begin{pmatrix} e^{i(\theta_s - \theta_{s-1})(m-1/2)} & 0 \\ 0 & e^{i(\theta_s - \theta_{s-1})(m+1/2)} \end{pmatrix}, \tag{14}$$

$$\mathcal{T}_M^{(s)} = \begin{pmatrix} \cos\Gamma_{nn',m}^{(s)} & -ie^{i\theta}\sin\Gamma_{nn',m}^{(s)} \\ -ie^{-i\theta}\sin\Gamma_{nn',m}^{(s)} & \cos\Gamma_{nn',m}^{(s)} \end{pmatrix}. \tag{15}$$

Note that these expressions are different from those from the Schrödinger counterpart. To carry out the analysis further, we have that the transfer matrix associated with the magnetic flux periodicity for $\theta = 0$ is given by

$$\mathcal{T}_\Phi = e^{i2\pi\Phi/\Phi_0}\mathcal{I}.$$

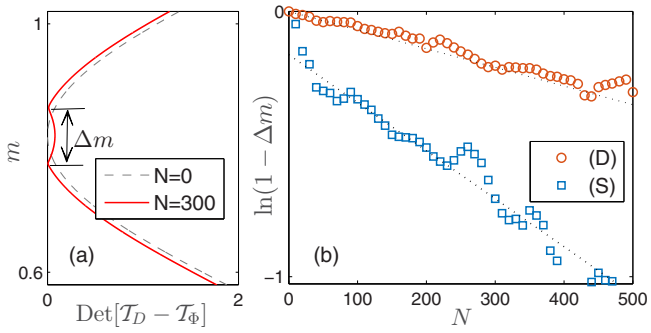

FIG. 7. For the Dirac ring domain, (a) the angular momentum quantum number m vs the value of the determinant of the transfer matrix, det$[T_D - T_\Phi]$, for two cases in which there is no disorder (dashed gray curves) and where there are 300 disorders (solid curves). (b) Decaying behavior of $1 - \Delta m$ with the number N of random disorders for Dirac ($u_m^{(D)} = 0.03$) and Schrödinger ($u_m^{(S)} = 0.075$) systems on a semilogarithmic scale.

Thus the relationship $m = m(\varepsilon)$ in the presence of random disorders can be solved when the transfer operator with disorder scattering can match the transfer matrix associated with the magnetic flux. We have

$$\det[\mathcal{T} - \mathcal{T}_\Phi] = 0. \tag{16}$$

In our heuristic analysis, we make the diagonal approximation, $n = n'$, so as to avoid generating any additional energy crossings [64].

Figure 7(a) shows the relation between the determinant of the difference of the transfer matrices $\det[\mathcal{T}_D - \mathcal{T}_\Phi]$ with the angular momentum quantum number m. In the absence of random disorders, Eq. (16) has a single solution, which corresponds to the energy crossing point. With random disorders, energy repulsion occurs, leading to a split in the original angular momentum quantum number, Δm, upon which the amplitude of the persistent current depends. Note that the range of Δm is [0,1]. For a small value of Δm, the energy repulsion is weak so that a large current can be maintained. On the contrary, for a large value of Δm the current amplitude becomes small. Roughly, the current amplitude is proportional to $1 - \Delta m$. Figure 7(b) shows the decreasing behavior of $1 - \Delta m$ on a semilogarithmic scale with the number of disorders. We see that the exponential decay rate is much smaller for the Dirac system than for the Schrödinger counterpart. For a relatively large value of N (e.g., $N \approx 400$), for the Dirac system the quantity $1 - \Delta m$ tends to plateau at a small (but nonzero) value, indicating a strong sustainability of the persistent currents against random disorders. In striking contrast, for the Schrödinger system, the value of $1 - \Delta m$ decays rapidly to zero, indicating that persistent currents in the nonrelativistic quantum ring are vulnerable to random disorders. These results are consistent with those from direct numerical calculations (Fig. 2).

Our analysis based on the quasi-1D equation provides a heuristic method to estimate the decay rate of the persistent currents as the number N (or density) of random disorders is increased. For an initial range of N, for both the Dirac and Schrödinger systems, the decaying behavior of the currents

can be written as $I_n/I_n^0 = A\exp(-\gamma N)$, where the decay rate is $\gamma \sim \langle\Gamma_n\rangle$, where Γ_n is the overlapping integral of the radial wave functions. Thus the ratio of the decay rates between the Dirac and Schrödinger systems is approximately given by

$$\frac{\gamma_n^{(D)}}{\gamma_n^{(S)}} \approx \frac{\langle\Gamma_n^{(D)}\rangle}{\langle\Gamma_n^{(S)}\rangle}, \tag{17}$$

where

$$\langle\Gamma_n^{(D)}\rangle = \int_\xi^1 dr\, \chi_n^{-*}\chi_n^+,$$

$$\langle\Gamma_n^{(S)}\rangle = \int_\xi^1 dr\, r\chi_n^{(S)*}\chi_n^{(S)}.$$

In the Dirac ring, the upper and lower components of the radial wave function have a large phase difference for low-energy levels, as shown in Figs. 6(b) and 6(c). As a result, we have

$$\langle\Gamma_n^{(D)}\rangle < \langle\Gamma_n^{(S)}\rangle.$$

For example, for the second and third energy levels, we have

$$\gamma_{2,3}^{(D)}/\gamma_{2,3}^{(S)} \approx \langle\Gamma_{2,3}^{(D)}\rangle/\langle\Gamma_{2,3}^{(S)}\rangle \approx 1/2,$$

which agrees approximately with the numerical results in Figs. 2(c) and 2(d). Note that this disorder-resistant scattering mechanism may be less effective for high-energy levels because the phase difference between the upper and lower components of the corresponding wave functions can be negligibly small. Consequently, the integral in Eq. (10) assumes values comparable to those in the Schrödinger ring system. The implication is that persistent currents associated with high-energy levels in the Dirac ring are expected not to be robust.

V. CONCLUSION AND DISCUSSION

For a ring domain with a magnetic flux through the center, persistent currents can arise due to the AB effect. This paper investigates the effect of random disorders on persistent currents in relativistic quantum (Dirac) ring systems. There are two reasons to investigate the impact of random disorders. First, in any realistic materials, random disorders are inevitable. In nonrelativistic quantum systems, the disorders have a devastating effect on the persistent currents, so they can only be observed in systems of sufficiently small size (e.g., size $\lesssim$ the phase coherence length of the material). For relativistic quantum systems, there is a recent work on the effects of random disorders on persistent currents in one dimension [62]. It is of interest to understand the effect in experimentally more feasible 2D systems. Secondly, in order to assess the feasibility of observing persistent currents in large systems, one can study the impact of random disorders of a systematically increasing density, because solving the Dirac equation under a magnetic field in a large system can be computationally demanding. These points can be elaborated on through the following discussion of the main results of this paper and their implications.

Previous theoretical and experimental results on persistent currents in nonrelativistic quantum (Schrödinger) systems revealed that the currents are sensitive and thus vulnerable to disorders. A natural question is then whether persistent currents can be more "sustainable" in relativistic quantum systems. Through direct numerical calculation of persistent currents for both Dirac and Schrödinger ring systems with systematically varying number (or density) of random disorders, we find that the currents in the Dirac system are significantly more robust than those in the Schrödinger counterpart. While for both systems, as the number of random disorders is increased from zero, the current amplitude decays exponentially, there are two key characteristic differences between the relativistic and nonrelativistic quantum cases. First, the rate of decay is much smaller in the Dirac than in the Schrödinger system. Secondly, for the Dirac ring the exponential decay is terminated when the number of random disorders becomes large and is subsequently replaced by a plateaued behavior with a finite current amplitude, but in the Schrödinger ring the exponential decay continues until the currents effectively become zero. The underlying quantum states providing "sustained" persistent currents in the Dirac system are found to be a WGM type of boundary states. We developed a physical theory, based on a quasi-1D approximation, to explain the distinct current decaying behaviors in the Dirac and Schrödinger systems. Specifically, under this approximation the effect of random disorders can be assessed and the persistent currents can be calculated through a scattering integral over the radial dimension that involves the product of the two components of the relativistic quantum spinor. These findings suggest the extraordinary robustness of persistent currents in the Dirac system, due to the robustness of the underpinnings of the currents, the WGM states, to random disorders.

Our calculations uncovered that, for both the Dirac and Schrödinger rings, the interior states are vulnerable to random disorders. It is the zero-flux boundary condition that renders the WGM boundary states robust in the Dirac system. (In the Schrödinger system, boundary states cannot form due to the Dirichlet boundary condition.) It is possible to observe the sustaining boundary states experimentally by exploiting, e.g., the surface states of a 3D topological insulators, where a ring domain can be formed through the deposition of ferromagnetic insulating materials on the surface of the topological insulator. Another finding is that the spin orientations of the WGM states are hardly affected by random disorders, which may have implications for relativistic quantum spintronic devices.

For the Dirac and Schrödinger systems, the energy dispersion relation is linear and parabolic, i.e., $E = k$ and $E = k^2$ (with a proper normalization), respectively. Under the normalization, the lowest energy level is larger than unity for both cases. For the same Fermi energy, the wavelength in the Dirac ring is smaller than that for Schrödinger counterpart. The robust persistent currents in the Dirac ring are thus not an effect of a larger wavelength and a weaker sensitivity to disorder. In fact, the robust persistent currents are due to the whispering gallery modes along the edges, as stipulated by the zero-flux boundary conditions in the Dirac ring.

An important implication of our finding lies in the possibility to observe persistent currents in Dirac systems of large sizes. In Schrödinger materials (normal metals or semiconductors), the currents can be observed but only when the device size is smaller than or close to the phase coherence length so that the electron trajectories are ballistic

or approximately ballistic with short diffusion time. When the device size is much larger than this scale, random scattering will be strong, diminishing the circulating current. However, the robustness of the persistent currents in the Dirac system implies that the relativistic quantum phenomenon can occur in larger devices, possibly on the macroscopic scale. This can be argued by noting that, as the ring size is increased, the number of scattering events that a particle experiences in one circulating motion will increase. From the standpoint of scattering, increasing the density of random disorders for fixed device size is equivalent to enlarging the device. For strong random disorders, Anderson localization sets in [70], prohibiting currents inside the domain. However, because of the strong boundary currents in Dirac fermion systems, it is possible that the persistent currents will not vanish. Below we provide an estimate of the maximally possible system size in which persistent currents can sustain.

In experimental studies, a 2D Dirac ring can be realized through the surface states of, e.g., Bi_2Te_3/Bi_2Se_3, with Fermi velocity about $v_F \approx 7 \times 10^5$ m/s [71–73]. In our simulation, the Gaussian-like disorder is analogous to charge puddles of size ∼30 nm and strength ∼10 meV associated with the surface states of Mn/Ca-doped Bi_2Te_3/Bi_2Se_3 materials [73]. In a pure Bi_2Te_3/Bi_2Se_3 sample, the strength of the charge puddles is smaller than that for doped materials. We can thus set $u_m/2 =$ 5 meV. In our computation, for the case of high disorder density, say 400–500 impurities, the disorder pattern is quite similar to that of the charge puddles from experiments [73]. The maximum strength of the charge puddles is given by $u_m = 300\Delta E_{10}$, with $\Delta E_{10} = \hbar v_F \Delta k_{10}/R_2$, where $k_{10}R_2 = 0.45$ and R_2 is the outer radius of the ring, which can be estimated as $R_2 = 300 \times 0.45\hbar v_F u_m \approx 6\ \mu$m. As a result, the estimated size of the Dirac ring in which robust persistent currents can exist is $D = 2R_2 \sim 12\ \mu$m, which is much larger than the maximum size of the normal metallic or semiconductor rings with persistent currents observed in previous experimental studies [6–13].

In a clean Dirac ring of size $D = 12\ \mu$m, the persistent currents associated with one energy level can be estimated as $I_n^0 \sim 2\Delta E_{10}/\Phi_0 = 0.45 \times \hbar v_F/(R_2\Phi_0) \approx 3$ nA, where $\Phi_0 = h/e \sim 4 \times 10^{-15}$ T m^2 is the magnetic flux quantum. Even if there are 500 impurities in the ring domain, there is still a finite persistent current: $I_n \approx 0.1 I_n^0 \approx 0.3$ nA. The total persistent current in an experimental system is given by $I = \sum_{n=1}^{N} I_n$, where the integer N depends on the Fermi energy. For example, if the Fermi energy is $E = 1$ meV, several energy levels will be included. The total persistent current is $I \sim 1$ nA, which can be observed in experiments, e.g., by using the SQUID technique [6–9,11,12].

ACKNOWLEDGMENTS

We thank H.-Y. Xu for valuable discussions. We would like to acknowledge support from the Vannevar Bush Faculty Fellowship program sponsored by the Basic Research Office of the Assistant Secretary of Defense for Research and Engineering and funded by the Office of Naval Research through Grant No. N00014-16-1-2828. This work was also supported by ONR under Grant No. N00014-15-1-2405.

APPENDIX A: ORTHONORMALITY OF RADIAL WAVE FUNCTIONS

The radial component of a Dirac spinor in two dimensions is governed by

$$\begin{pmatrix} 0 & \frac{d}{dr} + \frac{\bar{m}+1/2}{r} \\ -\frac{d}{dr} + \frac{\bar{m}-1/2}{r} & 0 \end{pmatrix} \chi = i\varepsilon\chi. \tag{A1}$$

The two decoupled equations for the upper and lower components of the radial wave function can be written as $H_r'\chi = 0$, where

$$\left[\frac{d^2}{dr^2} + \frac{1}{r}\frac{d}{dr} + \left(\varepsilon^2 - \frac{(\bar{m}-1/2)^2}{r^2}\right)\right]\chi_{n,m}^{-} = 0,$$
$$\left[\frac{d^2}{dr^2} + \frac{1}{r}\frac{d}{dr} + \left(\varepsilon^2 - \frac{(\bar{m}+1/2)^2}{r^2}\right)\right]\chi_{n,m}^{+} = 0. \tag{A2}$$

The solutions of these equations can be expressed in terms of the Hankel functions:

$$\begin{pmatrix} \chi_m^- \\ \chi_m^+ \end{pmatrix} = \frac{1}{\sqrt{N}} \begin{pmatrix} H_{\bar{m}-1/2}^{(1)}(\varepsilon r) + \alpha H_{\bar{m}-1/2}^{(2)}(\varepsilon r) \\ iH_{\bar{m}+1/2}^{(1)}(\varepsilon r) + i\alpha H_{\bar{m}+1/2}^{(2)}(\varepsilon r) \end{pmatrix}, \tag{A3}$$

where the coefficient α and the normalized coefficient N are given by

$$\begin{aligned} \alpha &= -\frac{H_{\bar{m}+1/2}^1(\varepsilon\xi) + H_{\bar{m}-1/2}^1(\varepsilon\xi)}{H_{\bar{m}+1/2}^2(\varepsilon\xi) + H_{\bar{m}-1/2}^2(\varepsilon\xi)} \\ &= -\frac{H_{\bar{m}+1/2}^1(\varepsilon) - H_{\bar{m}-1/2}^1(\varepsilon)}{H_{\bar{m}+1/2}^2(\varepsilon) - H_{\bar{m}-1/2}^2(\varepsilon)}, \\ N_m &= 2\pi \int_\xi^1 r\, dr(|\chi_m^{-\prime}|^2 + |\chi_m^{+\prime}|^2), \end{aligned} \tag{A4}$$

respectively, with $\chi_{1,2}'$ denoting the unnormalized radial wave functions. Consider two different pairs of quantum numbers: m_i, ε_i and m_j, ε_j, where $i \neq j$. Following a similar derivation method in Ref. [64] and using Eq. (A2), we obtain [64]

$$\begin{aligned} &\left(m_j^2 - m_i^2\right) \int_\xi^1 \frac{dr}{r} \chi_{m_j}^{\pm *}(r)\chi_{m_i}^{\pm}(r,\varepsilon_i) \\ &= \left(\varepsilon_j^2 - \varepsilon_i^2\right) \int_\xi^1 r\, dr\, \chi_{m_j}^{\pm *}(r,\varepsilon_j)\chi_{m_i}^{\pm}(r,\varepsilon_i). \end{aligned} \tag{A5}$$

Setting $\varepsilon_i = \varepsilon_j = \varepsilon$, we have $m_{i,j} = m_{i,j}(\varepsilon)$ and

$$\left[m_j^2(\varepsilon) - m_i^2(\varepsilon)\right] \int_\xi^1 \frac{dr}{r} \chi_{m_j(\varepsilon)}^{\pm *}(r,\varepsilon)\chi_{m_i(\varepsilon)}^{\pm}(r,\varepsilon) = 0. \tag{A6}$$

For nondegenerate energy levels, if $m_i(\varepsilon) \neq m_j(\varepsilon)$, the integral with the weight $1/r$ is zero. For $m_i(\varepsilon) = m_j(\varepsilon)$, the integral can assume an arbitrary value, and, for convenience, we can set it to be unity. As a result, the orthonormal condition becomes

$$\int_\xi^1 \frac{dr}{r} \chi_{m_j(\varepsilon)}^{\pm *}(r,\varepsilon)\chi_{m_i(\varepsilon)}^{\pm}(r,\varepsilon) = \delta_{i,j}, \tag{A7}$$

leading to the normalized condition

$$N_m^{\pm\prime} = 2\pi \int_\xi^1 \frac{dr}{r} |\chi_m^{\pm\prime}|^2. \tag{A8}$$

APPENDIX B: AZIMUTHAL EQUATION WITH RANDOM DISORDERS IN THE DIRAC RING SYSTEM

Substituting the entire wave function into the Dirac equation in the polar coordinates with random disorders [Eq. (2)], we have the equations for the upper and lower components of the spinor as

$$\phi^{+}_{n,m}\left(\partial_r + \frac{\Phi/\Phi_0}{r}\right)\chi^{+}_{n,m} - \chi^{+}_{n,m}\frac{i}{r}\partial_\theta\phi^{+}_{n,m} + ie^{i\theta}\phi^{-}_{n,m}(U_s-\varepsilon)\chi^{-}_{n,m} = 0,$$
$$\phi^{-}_{n,m}\left(\partial_r - \frac{\Phi/\Phi_0}{r}\right)\chi^{-}_{n,m} + \chi^{-}_{n,m}\frac{i}{r}\partial_\theta\phi^{-}_{n,m} + ie^{-i\theta}\phi^{+}_{n,m}(U_s-\varepsilon)\chi^{+}_{n,m} = 0. \tag{B1}$$

Since Eq. (A1) can be expressed as

$$\left(\partial_r + \frac{\Phi/\Phi_0}{r}\right)\chi^{+}_{n,m} = -\frac{m+1/2}{r}\chi^{+}_{n,m} + i\varepsilon\chi^{-}_{n,m} \text{ and } \left(\partial_r - \frac{\Phi/\Phi_0}{r}\right)\chi^{-}_{n,m}$$
$$= \frac{m-1/2}{r}\chi^{-}_{n,m} + i\varepsilon\chi^{+}_{n,m}, \tag{B2}$$

we can eliminate the term in the radial dimension: $\partial_r\chi^{\pm}$. In particular, making the approximation $e^{i\theta}\phi^{-}_{n} \approx \phi^{+}_{n}$, we can express the azimuthal equation in the matrix form as

$$\sum_n \frac{1}{r}\begin{pmatrix}\partial_\theta - i(m-1/2) & 0\\ 0 & \partial_\theta - i(m+1/2)\end{pmatrix}\begin{pmatrix}\phi^{-}_{n}\chi^{-}_{n,m}\\ \phi^{+}_{n}\chi^{+}_{n,m}\end{pmatrix} = \sum_n \begin{pmatrix}0 & e^{-i\theta}U_s(r,\theta)\\ e^{i\theta}U_s(r,\theta) & 0\end{pmatrix}\begin{pmatrix}\phi^{-}_{n}\chi^{-}_{n,m}\\ \phi^{+}_{n}\chi^{+}_{n,m}\end{pmatrix}. \tag{B3}$$

Multiplying $[\chi^{-*}_{n',m},\chi^{+*}_{n',m}]$ on both sides of Eq. (B3), integrating over r in the region $[\xi,1]$, and using the orthonormal condition in Eq. (A7), we can simplify the azimuthal equation for the Dirac system as

$$\begin{pmatrix}\partial_\theta - i(m-1/2) & 0\\ 0 & \partial_\theta + i(m+1/2)\end{pmatrix}\phi(\theta) = \sum_s\sum_{n'}\begin{pmatrix}0 & -e^{-i\theta}\int_\xi^1 dr\,\chi^{-*}_{n',m_s}{}^{U}(r,\theta)\chi^{+}_{n,m}\\ e^{i\theta}\int_\xi^1 dr\,\chi^{+*}_{n',m}U_s(r,\theta)\chi^{-}_{n,m} & 0\end{pmatrix}\phi. \tag{B4}$$

APPENDIX C: SCATTERING MATRIX METHOD FOR THE SCHRÖDINGER SYSTEM

Based on the same approximation as for the Dirac system, we have the azimuthal equation for the Schrödinger case as [64]

$$\left(\partial^2_\theta + m^2\right)\phi_n(\theta) = \sum_s\sum_{n'}\Gamma^{(s)}_{n'n,m}\phi_{n'}(\theta), \tag{C1}$$

where $\Gamma^{(s)}_{n'n,m} = u_s\chi^{*}_{n',m}(r_s)\chi_{n,m}(r_s)\delta(\theta-\theta_s)$. The orthonormal condition is [64]

$$\int_\xi^1 dr(1/r)\chi^{\dagger}_{m_j(\varepsilon)}(r,\varepsilon)\chi_{m_i(\varepsilon)}(r,\varepsilon) = \delta_{i,j}.$$

The azimuthal wave function of the Schrödinger system with an impulsive impurity satisfies the boundary conditions

$$\phi_n(\theta^{+}_s) = \phi_n(\theta^{-}_s),$$
$$\left.\frac{d\phi_n(\theta)}{d\theta}\right|_{\theta=\theta^{+}_s} - \left.\frac{d\phi_n(\theta)}{d\theta}\right|_{\theta=\theta^{-}_s} = \sum_{n'}\Gamma^{(s)}_{n'n,m}\phi_{n'}(\theta). \tag{C2}$$

Similar to the Dirac system, we make the diagonal approximation: $n = n'$. To avoid numerical divergence, we use the scattering matrix method. In particular, for propagation along a free path and scattering from an impurity, the respective scattering matrices can be obtained from Eq. (C2):

$$\mathcal{S}^{(s)}_P = \begin{pmatrix}0 & e^{i(\theta_s-\theta_{s-1})m}\\ e^{i(\theta_s-\theta_{s-1})m} & 0\end{pmatrix}, \tag{C3}$$

$$\mathcal{S}^{(s)}_M = \begin{pmatrix}-\frac{i\Gamma^{(s)}_{nn,m}e^{2im}}{2m-i\Gamma^{(s)}_{nn,m}} & \frac{2m}{2m-i\Gamma^{(s)}_{nn,m}}\\ \frac{2m}{2m-i\Gamma^{(s)}_{nn,m}} & -\frac{i\Gamma^{(s)}_{n,n}e^{-2im}}{2m-i\Gamma^{(s)}_{nn,m}}\end{pmatrix}. \tag{C4}$$

The total scattering matrix is given by

$$\mathcal{S} = \mathcal{S}^{(N+1)}_P \otimes \mathcal{S}^{(N)}_M \otimes \mathcal{S}^{(N)}_P \otimes \cdots \otimes \mathcal{S}^{(1)}_M \otimes \mathcal{S}^{(1)}_P. \tag{C5}$$

If we consider two scattering matrices defined by

$$\mathcal{S}_i = \begin{pmatrix}r_i & t'_i\\ t_i & r'_i\end{pmatrix}, \quad \mathcal{S}_j = \begin{pmatrix}r_j & t'_j\\ t_j & r'_j\end{pmatrix}, \tag{C6}$$

the compounded scattering matrix $\mathcal{S}_{ij} = \mathcal{S}_i \otimes \mathcal{S}_j$ can be calculated as [74–76]

$$\mathcal{S}_{ij} = \begin{pmatrix}r_i + t'_i r_j(1-r'_i r_j)^{-1}t_i & t'_i(1-r_j r'_i)^{-1}t_i\\ t_j(1-r'_i r_j)^{-1}t_i & r'_j + t_j r'_i(1-r_j r'_i)^{-1}t'_j\end{pmatrix}. \tag{C7}$$

Combining the total scattering matrix for a set of random disorders with the scattering matrix associated with the magnetic flux

$$\mathcal{S}_\Phi = \begin{pmatrix}0 & e^{-i2\pi\Phi/\Phi_0}\\ e^{i2\pi\Phi/\Phi_0} & 0\end{pmatrix}, \tag{C8}$$

we have [75,76]

$$\det[\mathcal{S} - \mathcal{S}_\Phi] = 0, \tag{C9}$$

from which the angular momentum quantum number m and its split value Δm can be solved.

[1] M. Büttiker, Y. Imry, and R. Landauer, Phys. Lett. A **96**, 365 (1983).
[2] Y. Aharonov and D. Bohm, Phys. Rev. **115**, 485 (1959).
[3] H.-F. Cheung, E. K. Riedel, and Y. Gefen, Phys. Rev. Lett. **62**, 587 (1989).
[4] A. Schmid, Phys. Rev. Lett. **66**, 80 (1991).
[5] H. Bouchiat, Physics **1**, 7 (2008).
[6] L. P. Lévy, G. Dolan, J. Dunsmuir, and H. Bouchiat, Phys. Rev. Lett. **64**, 2074 (1990).
[7] V. Chandrasekhar, R. A. Webb, M. J. Brady, M. B. Ketchen, W. J. Gallagher, and A. Kleinsasser, Phys. Rev. Lett. **67**, 3578 (1991).
[8] D. Mailly, C. Chapelier, and A. Benoit, Phys. Rev. Lett. **70**, 2020 (1993).
[9] W. Rabaud, L. Saminadayar, D. Mailly, K. Hasselbach, A. Benoît, and B. Etienne, Phys. Rev. Lett. **86**, 3124 (2001).
[10] N. A. J. M. Kleemans, I. M. A. Bominaar-Silkens, V. M. Fomin, V. N. Gladilin, D. Granados, A. G. Taboada, J. M. García, P. Offermans, U. Zeitler, P. C. M. Christianen, J. C. Maan, J. T. Devreese, and P. M. Koenraad, Phys. Rev. Lett. **99**, 146808 (2007).
[11] A. C. Bleszynski-Jayich, W. E. Shanks, B. Peaudecerf, E. Ginossar, F. von Oppen, L. Glazman, and J. G. E. Harris, Science **326**, 272 (2009).
[12] H. Bluhm, N. C. Koshnick, J. A. Bert, M. E. Huber, and K. A. Moler, Phys. Rev. Lett. **102**, 136802 (2009).
[13] M. A. Castellanos-Beltran, D. Q. Ngo, W. E. Shanks, A. B. Jayich, and J. G. E. Harris, Phys. Rev. Lett. **110**, 156801 (2013).
[14] H.-F. Cheung, Y. Gefen, E. K. Riedel, and W.-H. Shih, Phys. Rev. B **37**, 6050 (1988).
[15] F. von Oppen and E. K. Riedel, Phys. Rev. Lett. **66**, 84 (1991).
[16] J. F. Weisz, R. Kishore, and F. V. Kusmartsev, Phys. Rev. B **49**, 8126 (1994).
[17] T. Chakraborty and P. Pietiläinen, Phys. Rev. B **52**, 1932 (1995).
[18] Y. V. Pershin and C. Piermarocchi, Phys. Rev. B **72**, 125348 (2005).
[19] A. Bruno-Alfonso and A. Latgé, Phys. Rev. B **77**, 205303 (2008).
[20] H. Bary-Soroker, O. Entin-Wohlman, and Y. Imry, Phys. Rev. B **82**, 144202 (2010).
[21] K. S. Novoselov, A. K. Geim, S. V. Morozov, D. Jiang, Y. Zhang, S. V. Dubonos, I. V. Grigorieva, and A. A. Firsov, Science **306**, 666 (2004).
[22] C. Berger, Z. M. Song, T. B. Li, X. B. Li, A. Y. Ogbazghi, R. F. Z. T. Dai, A. N. Marchenkov, E. H. Conrad, P. N. First, and W. A. de Heer, J. Phys. Chem. B **108**, 19912 (2004).
[23] K. S. Novoselov, A. K. Geim, S. V. Morozov, D. Jiang, M. I. Katsnelson, I. V. Grigorieva, S. V. Dubonos, and A. A. Firsov, Nature (London) **438**, 197 (2005).
[24] Y. B. Zhang, Y. W. Tan, H. L. Stormer, and P. Kim, Nature (London) **438**, 201 (2005).
[25] A. H. Castro Neto, F. Guinea, N. M. R. Peres, K. S. Novoselov, and A. K. Geim, Rev. Mod. Phys. **81**, 109 (2009).
[26] N. M. R. Peres, Rev. Mod. Phys. **82**, 2673 (2010).
[27] S. D. Sarma, S. Adam, E. H. Hwang, and E. Rossi, Rev. Mod. Phys. **83**, 407 (2011).
[28] M. Z. Hasan and C. L. Kane, Rev. Mod. Phys. **82**, 3045 (2010).
[29] B. Radisavljevic, A. Radenovic, J. Brivio, V. Giacometti, and A. Kis, Nat. Nanotech. **6**, 147 (2011).
[30] Q. H. Wang, K. Kalantar-Zadeh, A. Kis, J. N. Coleman, and M. S. Strano, Nat. Nanotech. **7**, 699 (2012).
[31] D. Sheberla, L. Sun, M. A. Blood-Forsythe, C. R. W. S. Er, C. K. Brozek, A. Aspuru-Guzik, and M. Dinca, J. Am. Chem. Soc. **136**, 8859 (2014).
[32] S. M. Young, S. Zaheer, J. C. Y. Teo, C. L. Kane, E. J. Mele, and A. M. Rappe, Phys. Rev. Lett. **108**, 140405 (2012).
[33] Z. K. Liu, B. Zhou, Y. Zhang, Z. J. Wang, H. M. Weng, D. Prabhakaran, S.-K. Mo, Z. X. Shen, Z. Fang, X. Dai, Z. Hussain, and Y. L. Chen, Science **343**, 864 (2014).
[34] Z. K. Liu, J. Jiang, B. Zhou, Z. J. Wang, Y. Zhang, H. M. Weng, D. Prabhakaran, S.-K. Mo, H. Peng, P. Dudin, T. Kim, M. Hoesch, Z. Fang, X. Dai, Z. X. Shen, D. L. Feng, Z. Hussain, and Y. L. Chen, Nat. Mater. **13**, 677 (2014).
[35] S. M. Young and C. L. Kane, Phys. Rev. Lett. **115**, 126803 (2015).
[36] S.-K. Jian, Y.-F. Jiang, and H. Yao, Phys. Rev. Lett. **114**, 237001 (2015).
[37] H.-Y. Xu and Y.-C. Lai, Phys. Rev. B **94**, 165405 (2016).
[38] H. Xu and Y.-C. Lai, Phys. Rev. A **95**, 012119 (2017).
[39] A. H. Castro Neto, F. Guinea, and N. M. R. Peres, Phys. Rev. B **73**, 205408 (2006).
[40] D. S. L. Abergel, V. M. Apalkov, and T. Chakraborty, Phys. Rev. B **78**, 193405 (2008).
[41] C. W. J. Beenakker, A. R. Akhmerov, P. Recher, and J. Tworzydło, Phys. Rev. B **77**, 075409 (2008).
[42] M. Zarenia, J. M. Pereira, F. M. Peeters, and G. A. Farias, Nano Lett. **9**, 4088 (2009).
[43] R. Jackiw, A. I. Milstein, S.-Y. Pi, and I. S. Terekhov, Phys. Rev. B **80**, 033413 (2009).
[44] M. M. Ma, J. W. Ding, and N. Xu, Nanoscale **1**, 387 (2009).
[45] M. Zarenia, J. M. Pereira, A. Chaves, F. M. Peeters, and G. A. Farias, Phys. Rev. B **81**, 045431 (2010).
[46] D. Soriano and J. Fernández-Rossier, Phys. Rev. B **82**, 161302 (2010).
[47] D. Faria, A. Latgé, S. E. Ulloa, and N. Sandler, Phys. Rev. B **87**, 241403 (2013).
[48] N. Bolívar, E. Medina, and B. Berche, Phys. Rev. B **89**, 125413 (2014).
[49] P. Michetti and P. Recher, Phys. Rev. B **83**, 125420 (2011).
[50] D. Sticlet, B. Dóra, and J. Cayssol, Phys. Rev. B **88**, 205401 (2013).
[51] H. Xu, L. Huang, Y.-C. Lai, and C. Grebogi, Sci. Rep. **5**, 8963 (2015).
[52] H. Xu, L. Huang, and Y.-C. Lai, Europhys. Lett. **115**, 20005 (2016).
[53] J. U. Nöckel, A. D. Stone, G. Chen, H. L. Grossman, and R. K. Chang, Opt. Lett. **21**, 1609 (1996).
[54] C. Gmachl, F. Capasso, E. E. Narimanov, J. U. Nöckel, A. D. Stone, J. Faist, D. L. Sivco, and A. Y. Cho, Science **280**, 1556 (1998).
[55] S. M. Spillane, T. J. Kippenberg, and K. J. Vahala, Nature (London) **415**, 621 (2002).
[56] K. J. Vahala, Nature (London) **424**, 839 (2003).
[57] G. Reecht, H. Bulou, F. Scheurer, V. Speisser, B. Carrière, F. Mathevet, and G. Schull, Phys. Rev. Lett. **110**, 056802 (2013).
[58] M. V. Berry and R. J. Mondragon, Proc. R. Soc. London, Ser. A **412**, 53 (1987).
[59] P. Wei, F. Katmis, B. A. Assaf, H. Steinberg, P. Jarillo-Herrero, D. Heiman, and J. S. Moodera, Phys. Rev. Lett. **110**, 186807 (2013).
[60] E. K. Riedel and F. von Oppen, Phys. Rev. B **47**, 15449 (1993).

[61] M. I. Katsnelson, K. S. Novoselov, and A. K. Geim, Nat. Phys. **2**, 620 (2006).
[62] S. Ghosh and A. Saha, Eur. Phys. J. B **87**, 167 (2014).
[63] G. J. Ferreira and D. Loss, Phys. Rev. Lett. **111**, 106802 (2013).
[64] L. Wendler, V. M. Fomin, and A. A. Krokhin, Phys. Rev. B **50**, 4642 (1994).
[65] J. H. Bardarson, J. Tworzydło, P. W. Brouwer, and C. W. J. Beenakker, Phys. Rev. Lett. **99**, 106801 (2007).
[66] M. Titov, Europhys. Lett. **79**, 17004 (2007).
[67] F. Dominguez-Adame and E. Macia, J. Phys. A **22**, L419 (1989).
[68] F. Dominguez-Adame, Phys. Lett. A **159**, 153 (1991).
[69] C. L. Roy, Phys. Rev. A **47**, 3417 (1993).
[70] P. W. Anderson, Phys. Rev. **109**, 1492 (1958).
[71] H. Zhang, C.-X. Liu, X.-L. Qi, X. Dai, Z. Fang, and S.-C. Zhang, Nat. Phys. **5**, 438 (2009).
[72] Y. Xia, D. Qian, D. Hsieh, L. Wray, A. Pal, H. Lin, A. Bansil, D. Grauer, Y. S. Hor, R. J. Cava, and M. Z. Hasan, Nat. Phys. **5**, 398 (2009).
[73] H. Beidenkopf, P. Roushan, J. Seo, L. Gorman, I. Drozdov, Y. S. Hor, R. J. Cava, and A. Yazdani, Nat. Phys. **7**, 939 (2011).
[74] S. Datta, *Electronic Transport in Mesoscopic Systems* (Cambridge University Press, Cambridge, 1997).
[75] H. Tamura and T. Ando, Phys. Rev. B **44**, 1792 (1991).
[76] J. Feilhauer and M. Moško, Phys. Rev. B **84**, 085454 (2011).